



TRANSVERSE VIBRATION AND STABILITY PARAMETERS ANALYSES OF AN OFFSHORE FLUID-CONVEYING PIPE

¹Kuye S. I. and ²Olayiwola P. S.

¹Department of Mechanical Engineering, College of Engineering, Federal University of Agriculture, Abeokuta, Nigeria

²Department of Mechanical and Biomedical Engineering,
College of Engineering, Bells University, Ota, Nigeria

*Corresponding Email: ibiyemikuye@yahoo.com

Manuscript Received: 20/05/2018 Accepted: 30/06/2018 Published: September, 2018

ABSTRACT

The vibration and the stability behaviour of a simply supported offshore pipe conveying fluid was investigated in this research work. The governing differential equation for the transverse vibration of the system was derived according to Euler Bernoullis' equation for the fluid-pipe system and solved using the integral Fourier-Laplace Transformation. The effect of some flow parameters like mass ratios, Coriolis force and velocity of flow were analysed. The results revealed that natural frequency increased with increase in mass ratios and pipe thickness while it decreased with increase in pipe length. Flutter instability was observed in the system due to the presence of complex natural frequency where the imaginary part dominated the flow situation. The instability was made worse when Coriolis force was neglected.

Keywords: *Flow parameters, Coriolis force, natural frequency, stability.*

INTRODUCTION

Fluid conveying media are encountered almost on a daily basis either at homes or in the industry. Fluid conveyance attracts vibration as a result of the fluid moving from one end of the medium of conveyance to another. This vibration which can be mild and in some cases violent, depending on the nature of the fluid being conveyed and the properties of the medium of conveyance, can be detrimental if not well understood. Conveying pipes can be unstable at critical velocity leading to buckling (Paidoussis, 1998; Doares, 2010).

Vibrations have been reported in the past to be responsible for so many industrial accidents, collapse, dangerous leakages leading to explosions, high noise and even fire (Ibrahim, 2010). Resonance always occurs when the natural frequency of a vibrating system equals an exciting frequency leading to magnified vibrations which if not put under control can jeopardize the life of the system. Coriolis force which is a term of fluid conveyance has received several attentions over the years. While it is seen as countering the centrifugal effects by absorbing energy in such a way that the balance between the two parameters in the absence of dissipation gives rise to flutter, however, destabilization can occur under non-conservative forces (Olunloyo *et al.*, 2017).

The gyroscopic (Coriolis) forces, though, do no work in the course of free motions, they however have a strong influence on the overall dynamical behaviour of a pipeline system (Paidoussis, 2014).

Olunloyo *et al.*, (2007) studied the dynamics of offshore fluid conveying pipe and pipe walking phenomenon alongside the effect of elevated temperature. They concluded that there are significant contributions to pipe walking from other operating parameters rather than transient solution.

Environment of operations bearing in mind the possibility of excitations play a crucial role in the vibration of pipes. Pipes immersed in water respond differently from pipes suspended in the air. A buried pipe will not have the same excitation with the unburied and the depth of burial becomes very important in some cases.

Decrease in stiffness as a result of increase in flow speed is largely responsible for the instability of a pipe and the stiffness vanishes at the critical speed of flow (Paidoussis, 1998; Ibrahim, 2010). The instability which may be buckling or flutter may depend on some mechanical parameters and boundary conditions (Doares, 2010)

Al-Sahib *et al.*, (2010) investigated the stability of welded pipes both analytically and experimentally and concluded that clamped-clamped and clamped-pinned welded pipes conveying fluid are stable at small velocity but the clamped-pinned welded pipe loses stability at relatively high velocities.

Ibrahim (2010) reported that Jones and Goodwin (1971) in their work obtained the lower bounds for

the first Eigen values for low velocity thin pipe and showed that the Eigen values changed from real to imaginary as the fluid velocity increased through a critical flow velocity.

So many methods have been employed for beam problem analyses among which are those of Paidoussis and his co-workers who employed an Eigen function expansion in a modified Galerkin scheme (1998, 2000). The well known finite element method (Ibrahim, 2010), Several analytical methods (Olunloyo *et al.*, 2007), the boundary element method (Elfesoufi and Azrar, 2005), dual reciprocity method (Nardini and Brebbia, 1982) and integral methods (Olunloyo *et al.*, 2017) were also used by so many authors. Kutin and Bajsic (2014) employed smart materials and Jweeg and Ntayeesh (2015) made use of the application of method of multiple scales to analyze approximately the gyroscopic system for a nonlinear fluid-conveying pipeline.

The vibration and the dynamic stability of a simply supported offshore fluid-conveying pipe is considered in this work. The system being investigated consists of an elastic pipe of length L , internal cross-sectional area A , mass m_p and flexural rigidity EI , having an elastic foundation and conveying a fluid of mass m_f with a flow velocity U .

The following assumptions are considered in this research:

- (i) the pipeline is idealized as an elastic beam, simply supported and lying on subsoil layer modelled as a homogeneous infinite continuum.
- (ii) the flow is a fully developed pressurized incompressible viscous fluid.
- (iii) the dynamic system is under the influence of both internal and external loads with overlaying seawater pipeline interfacial frictional and drag forces.

MATERIALS AND METHODS

Governing Differential Equation and Problem Formulation

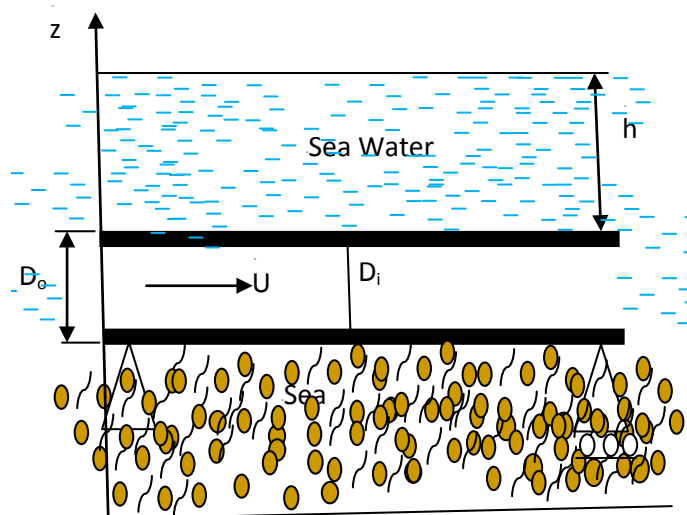


Fig. 1: A Model of Beam-Fluid System

Based on the assumptions listed above, the governing differential equation in the transverse direction is written according to Olunloyo *et al.*, (2007a) as

$$\left(EI \frac{\partial^4 w}{\partial x^4} - m \frac{\partial^2 w}{\partial t^2} + m_f U^2 \frac{\partial^2 w}{\partial x^2} + 2m_f U \frac{\partial^2 w}{\partial t \partial x} + \rho A \frac{\partial^2 w}{\partial x^2} + c \frac{\partial w}{\partial t} \right) \left(c_s \frac{\partial w}{\partial t} + k_s w = \left(\frac{\partial \phi}{\partial t} + gz \right) \rho A_s \right) \dots\dots\dots(1)$$

Non-dimensionalization of Eq. (1) leads to

$$\left(\frac{\partial^4 \bar{w}}{\partial \bar{x}^4} + \frac{\partial^2 \bar{w}}{\partial \bar{t}^2} + (\delta U^2 + \bar{p}A) \frac{\partial^2 \bar{w}}{\partial \bar{x}^2} + \delta U \frac{\partial^2 \bar{w}}{\partial \bar{t} \partial \bar{x}} + \bar{p}A \frac{\partial^2 \bar{w}}{\partial \bar{x}^2} + c \frac{\partial \bar{w}}{\partial \bar{t}} \right) \left(-c_s \frac{\partial \bar{w}}{\partial \bar{t}} + \bar{k}_s \bar{w} - \left(\beta_1 \frac{\partial \bar{\phi}}{\partial \bar{t}} + \beta_2 \bar{z} \right) \bar{A}_s \right) \dots\dots\dots(2)$$

where,

$$\bar{x} = \frac{x}{L}, \bar{w} = \frac{w}{L}, \delta = \frac{m_f}{m}, \bar{p}A = \frac{\rho A L^2}{EI}, c = \frac{c L^2}{\sqrt{EI m}}, c_s = \frac{c_s L^2}{\sqrt{EI m}}, \bar{k}_s = \frac{k_s L^2}{EI}, \bar{t} = \frac{t}{L^2} \sqrt{\frac{EI}{m}}, U = UL \sqrt{\frac{m}{EI}}, \beta_1 = \frac{2\pi r_s \rho_s L^2}{\sqrt{EI m}}, \beta_2 = \frac{2\pi g r_s \rho_s L^3}{EI}, \bar{A}_s = \frac{A_s}{L^2} \dots\dots\dots(3)$$

Analysis of the Governing Equation

Introducing Laplace transform namely

$$(\bar{\cdot}) = \frac{1}{2\pi i} \int_{\gamma - i\infty}^{\gamma + i\infty} (\cdot) e^{st} dt; (\cdot) = \frac{1}{2\pi i} \int_{\gamma - i\infty}^{\gamma + i\infty} (\bar{\cdot}) e^{-st} ds \dots\dots\dots(4)$$

to Eq. (2) and applying initial conditions namely

$$\bar{w}(\bar{x}, 0) = 0, \frac{d\bar{w}}{d\bar{x}}(\bar{x}, 0) = 0 \dots\dots\dots(5)$$

gives

$$\left(\frac{d^4 \bar{w}}{d\bar{x}^4} + s^2 \bar{w} + (\delta U^2 + \bar{p}A) \frac{d^2 \bar{w}}{d\bar{x}^2} + \delta U s \frac{d\bar{w}}{d\bar{x}} + \bar{c} s \bar{w} + \bar{c}_s s \bar{w} + k_s \bar{w} \right) = \left(\beta_1 s \bar{\phi} + \frac{\beta_2 \bar{z}}{s} \right) \bar{A}_s \dots\dots\dots(6)$$

Applying Fourier complex integral transforms according to Wrede and Spiegel (2002), Jeffrey (2002), Olayiwola (2016) and Olunloyo *et al.* (2017) namely:

$$\begin{aligned} \mathcal{F}^{-1} \left\{ \frac{1}{\sqrt{2\pi}} \int_{-\infty}^{\infty} \bar{w}(\bar{x}, \bar{t}) e^{-i\bar{k}\bar{x}} d\bar{x} \right\} &= \bar{w}^F(\bar{x}, \bar{t}) \\ \mathcal{F}^{-1} \left\{ \frac{1}{\sqrt{2\pi}} \int_{-\infty}^{\infty} \bar{w}^F(\bar{x}, \bar{t}) e^{i\bar{k}\bar{x}} d\bar{k} \right\} &= w(x, t) \\ \mathcal{F}(w, \bar{t}) &= \begin{cases} 0 & \text{when } -\infty \leq x < 0 \\ w(x, \bar{t}) & \text{when } 0 < x < L \\ 0 & \text{when } L < x < \infty \end{cases} \dots\dots\dots(7) \end{aligned}$$

$$\left(n^4 \bar{w}^F + \frac{d^2 \bar{w}^F}{d\bar{x}^2} e^{-i\bar{k}\bar{x}} \Big|_0^L + i n \frac{d^2 \bar{w}^F}{d\bar{x}^2} e^{-i\bar{k}\bar{x}} \Big|_0^L - n^2 \frac{d\bar{w}^F}{d\bar{x}} e^{-i\bar{k}\bar{x}} \Big|_0^L - i n^3 \bar{w}^F e^{-i\bar{k}\bar{x}} \Big|_0^L \right) \left(\delta U^2 + \bar{p}A \right) n^2 \bar{w}^F + \left(\delta U^2 + \bar{p}A \right) \frac{d\bar{w}^F}{d\bar{x}} e^{-i\bar{k}\bar{x}} \Big|_0^L + i n \bar{w}^F e^{-i\bar{k}\bar{x}} \Big|_0^L - 2ins\delta U \bar{w}^F + 2\delta U \bar{w}^F e^{-i\bar{k}\bar{x}} \Big|_0^L + s^2 \bar{w}^F + \bar{c} s \bar{w}^F + k_s \bar{w}^F = -\beta_1 s \bar{\phi} - \frac{\beta_2 \bar{z}^F}{s} \dots\dots\dots(8)$$

Applying the classical boundary conditions for a simply supported beam namely

$$\begin{aligned} \bar{w}(\bar{x}, \bar{t}) = \frac{d^2 \bar{w}}{d\bar{x}^2}(\bar{x}, \bar{t}) = 0 \\ \bar{w}(\bar{x}, \bar{t}) = \frac{d^2 \bar{w}}{d\bar{x}^2}(\bar{x}, \bar{t}) = 0 \end{aligned} \dots\dots\dots(9)$$

Eq. (8) becomes

$$\left(\left(n^4 - (\delta U^2 + \bar{p}A) \right) n^2 + s(c + 2in\delta U) \right) \bar{w}^F = \Phi - \beta_1 s \bar{\phi} - \frac{\beta_2 \bar{z}^F}{s} \left(-s^2 \left(-\bar{\beta} \beta_1 \right) - \bar{c} s \bar{w}^F + k_s \right) \dots\dots\dots(10)$$

where,

$$\Phi = n^2 \frac{d\bar{w}^F}{d\bar{x}} e^{-i\bar{k}\bar{x}} \Big|_0^L - \frac{d^2 \bar{w}^F}{d\bar{x}^2} e^{-i\bar{k}\bar{x}} \Big|_0^L - (\delta U^2 + \bar{p}A) \frac{d\bar{w}^F}{d\bar{x}} e^{-i\bar{k}\bar{x}} \Big|_0^L \dots\dots\dots(11)$$

But according to Olunloyo *et al.*,(2007a)

$$\bar{\phi} = \bar{\beta} s \bar{w}^F(\bar{x}_s, \bar{t}), \bar{\beta} = \frac{-\bar{v}_s \cosh(\bar{k}\bar{z})}{\bar{k} \sinh(\bar{k}h)}, \bar{k} = \frac{n\pi}{\bar{\lambda}} \dots\dots\dots(12)$$

The static solution of a simply supported pipe given by

$$w = \frac{\sigma_1 z^3}{2EI} \left(-\frac{\bar{x}^3}{24} - \frac{\bar{x}^2}{12} - \frac{\bar{x}}{24} \right) \dots\dots\dots(13)$$

which representing the condition of no fluid in the pipe can then be employed for the solution of Eq. (11) giving

$$\Phi = \frac{p}{EI} \left(\frac{1}{2} (-2\bar{x} + 1) - (n^2 - \delta U^2) \left(\frac{4x^3 + 2x^2 - 1}{24} \right) \right) e^{-i\bar{k}\bar{x}} \Big|_0^L \dots\dots\dots(14)$$

Substituting Eq. (12) into Eq. (10) leads to

$$\left(\left(n^4 - (\delta U^2 + \bar{p}A) \right) n^2 + s(c + 2in\delta U) \right) \bar{w}^F = \Phi - \frac{\beta_2 \bar{z}^F}{s} \left(-s^2 \left(+\bar{\beta} \beta_1 \right) - \bar{c} s \bar{w}^F + k_s \right) \dots\dots\dots(15)$$

$$\left(1 + \bar{\beta} \beta_1 \right) s^2 + s\Lambda_1 + \Lambda^2 \bar{w}^F = \Phi - \frac{\beta_2 \bar{z}^F}{s} \dots\dots\dots(16)$$

$$\bar{w}^F = \frac{-\beta_2 \bar{z}^F + \Phi}{\left(1 + \bar{\beta} \beta_1 \right) \left(s^2 + s\Lambda_1 + \Lambda^2 \right)} \dots\dots\dots(17)$$

$$\bar{w}^F = \frac{-\beta_2 \bar{z}^F}{\left(1 + \bar{\beta} \beta_1 \right) \left(s^2 + s\Lambda_1 + \Lambda^2 \right)} + \frac{\Phi}{\left(1 + \bar{\beta} \beta_1 \right) \left(s^2 + s\Lambda_1 + \Lambda^2 \right)} \dots\dots\dots(18)$$

where,

$$\begin{aligned} \Lambda_1 &= \frac{\bar{c} + 2in\delta U}{1 + \bar{\beta} \beta_1} \\ \Lambda^2 &= \frac{n^4 - \delta U^2 n^2 + k_s}{1 + \bar{\beta} \beta_1} \end{aligned} \dots\dots\dots(19)$$

Analysis of the Natural Frequencies

Using the characteristic equation in Eq.(18) to obtain the natural frequencies of the system leads to

$$s^2 + sA_1 + A^2 = 0 \quad \dots\dots(20)$$

Eq. (22) can be written as

$$(s + \zeta_1)(s + \zeta_2) = 0 \quad \dots\dots(21)$$

where,

$$\begin{aligned} \zeta_1 &= \frac{-A_1}{2} + i\sqrt{A^2 - \frac{A_1^2}{4}} \\ \zeta_2 &= \frac{-A_1}{2} - i\sqrt{A^2 - \frac{A_1^2}{4}} \end{aligned} \quad \dots\dots(22)$$

The dimensionless natural frequencies for the system can be computed from Eq. (21) as follows

Let $\Psi = -H\Phi_{11} \dots\dots (23)$

Eq. (21) then becomes

$$\begin{aligned} (i\omega_n)^2 + i\omega_n A_1 + A^2 &= 0 \\ -\omega_n^2 - i\omega_n A_1 + A^2 &= 0 \\ \omega_n^2 + i\omega_n A_1 - A^2 &= 0 \\ \omega_{1,2} &= \frac{-iA_1 \pm \sqrt{(A_1)^2 - 4A^2}}{2} \end{aligned} \quad \dots\dots(24)$$

Eq. (24) gives the natural frequencies of the system

Analysis of the Dynamic Stability

Let us consider Eq. (22) again, where,

$$\begin{aligned} \zeta_1 &= \frac{-A_1}{2} + i\sqrt{A^2 - \frac{A_1^2}{4}} \\ \zeta_2 &= \frac{-A_1}{2} - i\sqrt{A^2 - \frac{A_1^2}{4}} \end{aligned}$$

The poles of the system are given by the roots of the characteristic equation in Eq. 22.

The system is said to be stable when the characteristic equation has negative roots ζ_1 and ζ_2 (Ibrahim, 2010, Jone and Goodwin, 1971). The real parts of the conjugate pairs of the complex roots illustrate the stability while the imaginary parts illustrate the damping. The higher the values on the imaginary parts the lower the damping of the system (Paidousis and Issid, 1974). Argand diagram of the system is drawn using the real and imaginary parts of the poles $Re(\zeta_1)$, $Im(\zeta_1)$, $Re(\zeta_2)$ and $Im(\zeta_2)$ with the flow velocity, v , as the parameter.

Analysis of the Dynamic Response

Fourier-Laplace inversion of Eq. (18) gives the response of the system and it is written as

$$\bar{w}(\bar{x}, \bar{t}) = \sum_{n=1}^{\infty} B e^{s_n t} \quad \dots\dots(25)$$

where,

$$B = \int_0^1 \bar{w}(\bar{x}, \bar{t}) e^{-i\lambda \bar{x}} d\bar{x} \quad \dots\dots(26)$$

Therefore,

$$\bar{w}(\bar{x}, \bar{t}) = \left(\frac{-\beta_2 z \Xi(\bar{x}) \Psi_1(\bar{t})}{(+\beta \beta_1)} \right) \left(\frac{x^4}{24} + \frac{x^3}{12} - \frac{x}{24} \right) \sum_{n=1}^{\infty} \frac{\hat{\Phi} \Psi_n(\bar{t})}{(-\beta \beta_1)} e^{s_n t} \quad \dots\dots(27)$$

but $z = -h$, therefore

$$\bar{w}(x, t) = \left(\frac{\beta_2 h \Xi(\bar{x}) \Psi_1(\bar{t})}{(+\beta \beta_1)} \right) \left(-\frac{x^4}{24} + \frac{x^3}{12} - \frac{x}{24} \right) \sum_{n=1}^{\infty} \frac{\hat{\Phi} \Psi_n(\bar{t})}{(+\beta \beta_1)} e^{s_n t} \quad \dots\dots(28)$$

where,

$$\begin{aligned} \Psi &= \begin{pmatrix} 1 & e^{-\zeta_1 t} & e^{-\zeta_2 t} \\ \zeta_1 - \zeta_2 & \zeta_2 (\zeta_1 - \zeta_2) & \zeta_1 (\zeta_1 - \zeta_2) \end{pmatrix} \\ \Psi_1 &= \begin{pmatrix} e^{-\zeta_1 t} & e^{-\zeta_2 t} \\ \zeta_2 & -\zeta_1 \end{pmatrix} \\ \Xi(\bar{x}) &= \frac{\bar{x}^3}{12} - \frac{\bar{x}^2}{24} - \frac{\bar{x}}{24} \\ \hat{\Phi} &= \frac{P}{24EI} \left((v^2 \pi^2 - 8U^2 - 4) e^{-i\pi x} - (v^2 \pi^2 - 8U^2 + 12) \right) \end{aligned} \quad \dots\dots(29)$$

RESULTS AND DISCUSSION

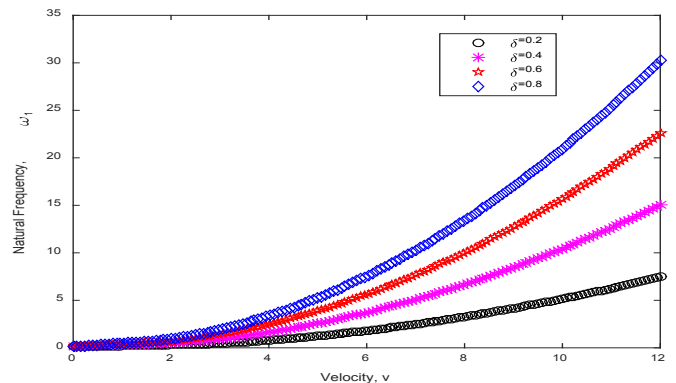


Figure 2: Natural frequency (ω_1) profile as a function of delta for the case

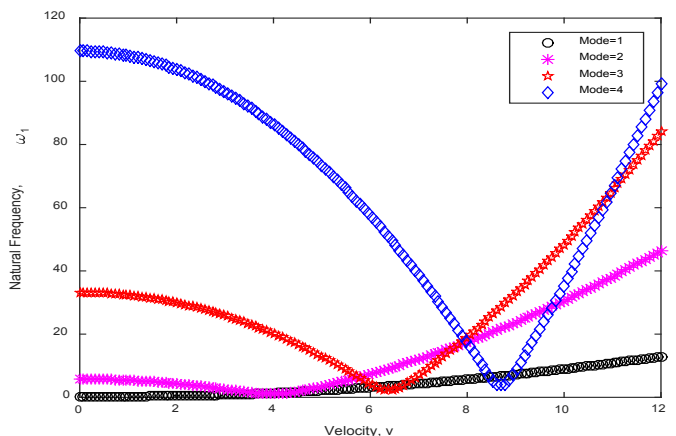


Figure 3: Natural frequency (ω_1) profile as a function of mode for the case $L = 150$ m, $h = 100$ m, $\delta = 0.2$

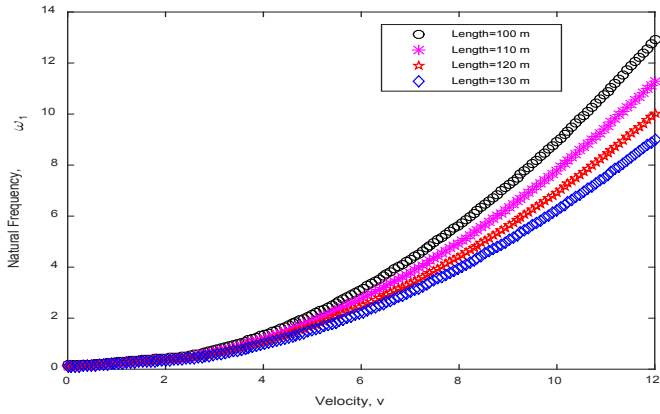


Figure 4: Natural frequency (ω_1) profile as a function of L for the case $\delta = 0.2, h = 100 \text{ m}, n = 1$

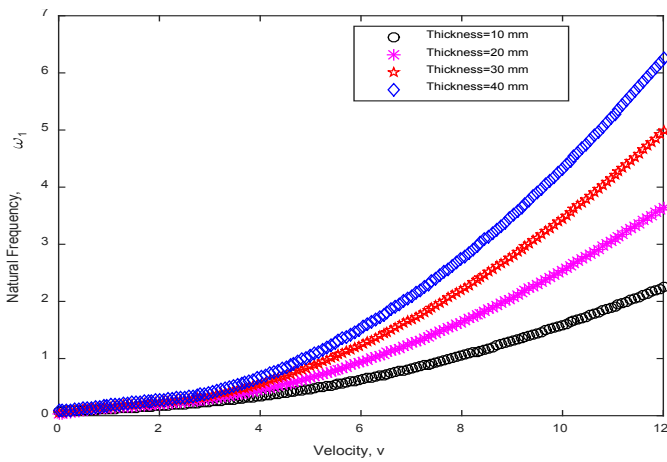


Figure 5: Natural frequency (ω_1) profile as a function of pipe thickness for the case $L = 150 \text{ m}, h = 100 \text{ m}, n = 1$

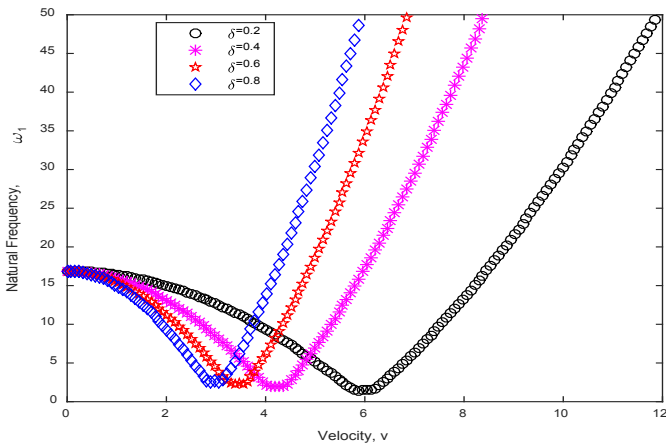


Figure 6: Natural frequency (ω_1) profile as a function of δ for the case $L = 150 \text{ m}, h = 100 \text{ m}, n = 3$

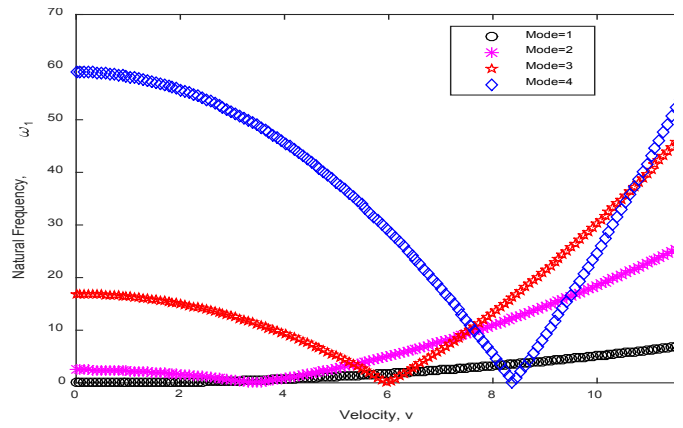


Figure 7: Natural frequency (ω_1) profile as a function of δ in the absence of Coriolis effect for the case $L = 150 \text{ m}, h = 100 \text{ m}, \delta = 0.2$

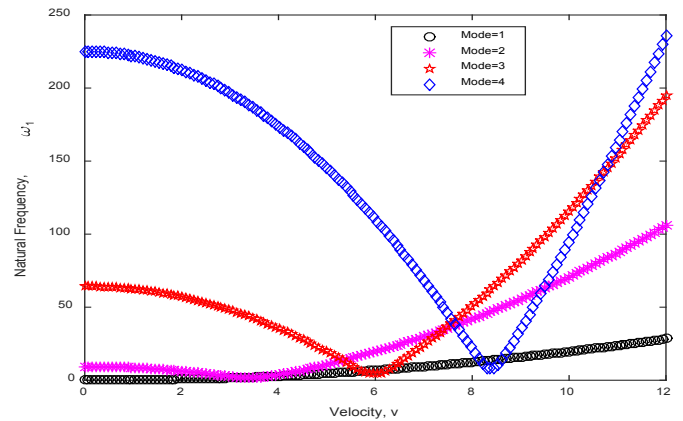


Figure 8: Natural frequency (ω_1) profile as a function of mode without seawave effect for the case $L = 150 \text{ m}, h = 100 \text{ m}, \delta = 0.2$

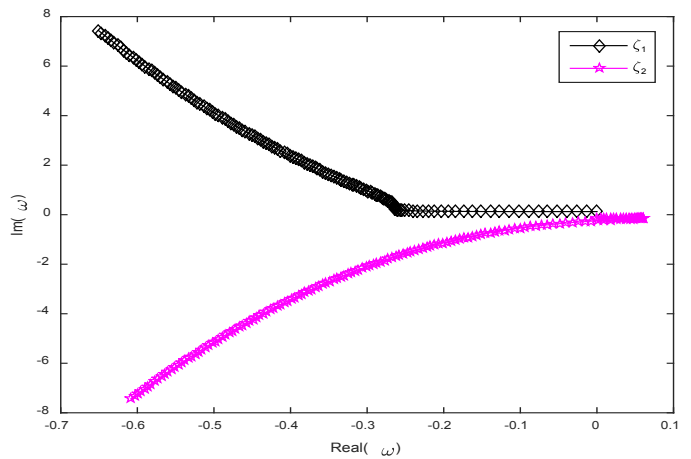


Figure 9: Imaginary natural frequency versus real Natural frequency as a function of poles for the case $L = 150 \text{ m}, h = 100 \text{ m}, n = 1, \delta = 0.2$

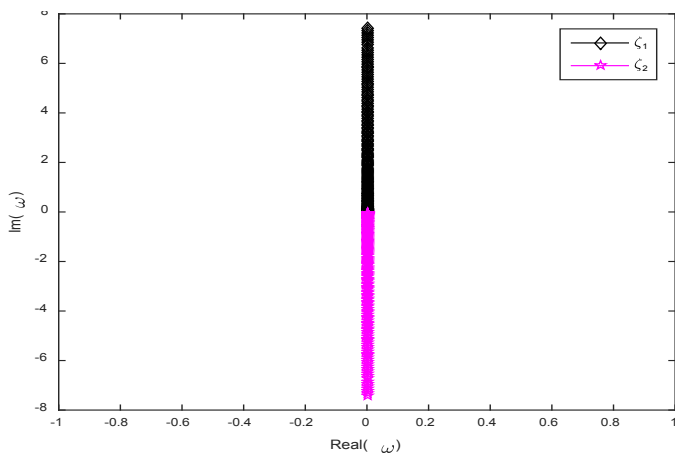


Figure 10: Imaginary natural frequency versus real Natural frequency in the absence of Coriolis as a function of poles for the case

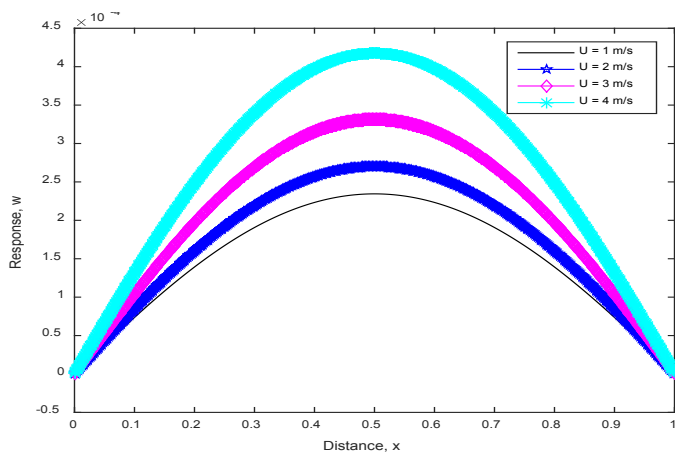


Figure 11: Dynamic response (w) as a function of flow velocity for the case

The computations were done using 100 m long steel pipe with radius 0.4m, thickness 10 mm, density 7850 kg/m³, conveying a fluid of density 977 kg/m³, submerged in seawater with density 1025 kg/m³. From the results of the analysis carried, Fig. 2 shows the graph of natural frequency against the velocity of flow for different mass ratios. It can be seen from the graph that the natural frequency is very low at the beginning of the curve indicating that the system's critical velocity is very low at the onset of flow after which the natural frequency rises again.

The graph of natural frequency against velocity of flow for different modes shown in Fig.3 reveals that the graph has two parts, firstly, natural frequency starts at some value and decreases with the velocity of flow till the lowest value after which it rises again. Natural frequency and the critical velocity in this case increase with modes with the lowest mode having the lowest starting natural frequency. Fig.4 has a similar profile with Fig.3 and that is because the lowest mode is considered. Natural frequency follows the same pattern as Fig.3 with the values decreasing with

increase in pipe length. Effect of pipe thickness is showcased in Fig. 5 where a similar pattern with Fig.4 can be seen. Here, natural frequency increases with pipe thickness, meaning, thinner pipes will vibrate more because they possess lower flexural rigidity.

Fig. 6 is the curve of natural frequency against flow velocity for different mass-ratios for mode 3. Here, the natural frequency can be seen to start at higher values, and decreased to the lowest values before rising again. The effect of the absence of Coriolis force can be seen in Fig. 7, lower natural frequencies were obtained for all the modes considered compared with those of Fig. 2 which agrees with Plaut (2006) that Coriolis force does work. Fig.8 gives the curve of natural frequency against the flow velocity in the absence of sea-wave (when the sea is assumed calm). Natural frequency in this case is relatively high compared with those obtained in Figs. 3 and 7. It can be seen that, the natural frequency of the system is highly influenced by the sea waves as increase in natural frequency was observed in the absence of sea waves.

The Argand diagrams of the system are given by Figs. 9 and 10, showing the complex poles of the system represented by the first and the complimentary natural frequencies drawn with the real parts on the horizontal axis and the imaginary parts on the vertical axis. The poles are mirror images about the real axis. Fig. 9 has the presence of Coriolis, and the two poles having initial real values diverged into imaginary plane after some time. It follows that if a pole lies on the negative real axis, the vibration will die away and if it lies on the positive real axis, the vibration will grow. According to Ibrahim (2010), higher imaginary values increase oscillation of the system. It is observed that when the Coriolis effect is ignored as in Fig.10, the poles are highly influenced by the values on the imaginary plane leading to instability. But, with Coriolis, the poles lie in the negative real axis which shows that Coriolis contributes to the stability of the system. This agrees with the argument of Paidoussis (2014) on the role of Coriolis force. The dynamic response of the system as a function of velocity is illustrated in Fig. 11 showing that deformation increases with flow velocity.

CONCLUSION

This work investigated the dynamic vibration and stability of a fluid-conveying offshore pipeline system. Euler Bernoulli equation for the system was analysed and solved with the aids of Fourier-Laplace Transformation and the effects of important parameters like mass ratios, Coriolis force, pipe length and thickness were equally analysed. Coriolis force played a significant role on the stability of the system.

REFERENCES

- Amabili M., Pellicano F. and Paidoussis M.P. (2000). Non-linear dynamics and stability of circular cylindrical shells containing flowing fluid, Part IV: large-amplitude vibrations with flow, *Journal of Sound and Vibration*, Vol. 237, pp 641-666.
- Bou-Rabee, N. M. (2002). Numerical stability analysis of a tubular cantilevered conveying fluid, *California Institute of Technology*.
- Doares, O. (2010), Dissipation effect on local and global stability of fluid-conveying pipes, *Journal of Sound and Vibration*, Vol. 329, pp 72–83
- Elfelsoufi, Z., Azrar, L. (2005). Buckling, Flutter and Vibration Analyses of Beams by Integral Equation Formulations, *Computer and Structures*, vol. 83, pp 2632-2649.
- Ibrahim, R. A. (2010). Overview of Mechanics of Pipes Conveying Fluids—Part I: *Fundamental Studies*, *Journal of Pressure Vessel Technology*, Vol. 132 / 034001-1
- Jeffrey, A. (2002). *Advanced Engineering Mathematics*, Harcourt Academic Press, Burlington, Mass, USA. View at Math Sci Net
- Jones, L. H., and Goodwin, B. E. (1971). The Transverse Vibrations of a Pipe Containing Flowing Fluid: Methods of Integral Equations, *Q. Appl. Math.*, Vol. 29, pp. 363–374.
- Jweeg, M. J., Ntayeesh, T. J. (2015). Dynamic analysis of pipes conveying fluid using analytical, numerical and experimental verification with the aid of smart materials, *International Journal of Science and Research*, vol. 4, no. 12, 2015.
- Kutin, J., Bajsić, I. (2014). Fluid-dynamic loading of pipes conveying fluid with a laminar mean-flow velocity profile, *Journal of Fluids and Structures*, vol. 50, pp. 171–183.
- Lee S. I. and Chung J. (2002). New non-linear modeling for vibration analysis of a straight pipe conveying fluid, *Journal of Sound and Vibration*, Vol. 254, pp 313-325.
- Manabe T., Tosaka N. and Honama T. (1999). Dynamic stability analysis of flow-conveying pipe with two lumped masses by domain decomposition beam, *Fuji Research Institute Corp.*, Tokyo, Japan.
- Nabeel K. Abid Al-Sahib, Adnan N. Jameel, Osamah F. Abdulateef (2010). Investigation into the Vibration Characteristics and Stability of a Welded Pipe Conveying Fluid, *Jordan Journal of Mechanical and Industrial Engineering*, Vol. 4, No 3, ISSN 1995-6665 Pp 378 – 387.
- Nardini, D., Brebbia, C. A. (1982). A new approach to free vibration analysis using boundary element method, *Springer*, 1982, pp 313-326.
- Olayiwola, P. S. (2016). Mechanics of a fluid-conveying pipeline system resting on a viscoelastic foundation, *Journal of Multidisciplinary Engineering Science Studies (JMESS)*, Vol. 2, no. 3. View at Google Scholar
- Olunloyo, V. O. S., Oyediran, A., Adewale, A., Adelaja, A. O. and Osheku, C. A. (2007a). Concerning the Transverse and Longitudinal Vibrations of A Fluid Conveying Beam and the Pipe Walking Phenomenon. *Proceedings 26th ASME International Conference on Offshore Mechanics and Arctic Engineering-OMAE*, Vol. 3, no. OMAE2007-29304, pp.285-298.
- Olunloyo, V. O. S., Osheku, C. A. and Oyediran, A. A. (2007b). Dynamic Response Interaction of Vibrating Offshore Pipeline on Moving Seabed. *ASME Journal of Offshore Mechanics and Arctic Engineering* Vol. 129 (2), pp 107-119.
- Olunloyo, V. O. S., Osheku, C. A., and Olayiwola, P. S. (2017). A Note on an Analytic Solution for an Incompressible Fluid-Conveying Pipeline System, *Advances in Acoustics and Vibration*, Vol. 2017 (2017), Article ID 8141523, 20 pages <https://doi.org/10.1155/2017/8141523>
- Paidoussis, M. P. (1998). Fluid-structure Interactions, *Slender Structures and Axial Flow*, Vol. 1, Academic Press, New York.
- Paidoussis, M. P. (2014). Fluid-Structure Interactions: *Slender Structures and Axial Flows*, Vol. 1, Academic Press.
- Plaut, R. H. (2006). Post buckling and Vibration of End-Supported Elastica Pipes Conveying Fluid and Columns Under Follower Loads, *Journal of Sound and Vibration*, Vol.289 (1–2), pp. 264–277.
- Wrede, R. C. and Spiegel, M. (2002). *Theory and Problems of Advanced Calculus*, Schaum's Outline Series, McGraw-Hill, New York, NY, USA, 2nd edition.